



ULUSLARARASI 3B YAZICI TEKNOLOJİLERİ
VE DİJİTAL ENDÜSTRİ DERGİSİ

INTERNATIONAL JOURNAL OF 3D PRINTING
TECHNOLOGIES AND DIGITAL INDUSTRY

ISSN:2602-3350 (Online)

URL: <https://dergipark.org.tr/ij3dptdi>

EFFECT OF PRINTING SPEED ON FDM 3D-PRINTED PLA SAMPLES PRODUCED USING DIFFERENT TWO PRINTERS

Yazarlar (Authors): Muhammed Safa Kamer^{ID*}, Semsettin Temiz^{ID}, Hakan Yaykasli^{ID}, Ahmet Kaya^{ID}, Orhan Erdal Akay^{ID}

Bu makaleye şu şekilde atıfta bulunabilirsiniz (To cite to this article): Kamer M.S., Temiz S., Yaykasli H., Kaya A., Akay O.E., “Effect of Printing Speed On FDM 3D-Printed PLA Samples Produced Using Different Two Printers” *Int. J. of 3D Printing Tech. Dig. Ind.*, 6(3): 438-448, (2022).

DOI: 10.46519/ij3dptdi.1088805

Araştırma Makale/ Research Article

Erişim Linki: (To link to this article): <https://dergipark.org.tr/en/pub/ij3dptdi/archive>

EFFECT OF PRINTING SPEED ON FDM 3D-PRINTED PLA SAMPLES PRODUCED USING DIFFERENT TWO PRINTERS

Muhammed Safa Kamer^a ^{*}, Semsettin Temiz^b , Hakan Yaykasli^c , Ahmet Kaya^a , Orhan Erdal Akay^a 

^aKahramanmaraş Sutcu Imam University, Faculty of Engineering and Architecture, Department of Mechanical Engineering, TURKEY

^bInonu University, Faculty of Engineering, Department of Mechanical Engineering, TURKEY

^cKahramanmaraş Istiklal University, Elbistan Vocational School of Higher Education, Department of Electronics Technology, TURKEY

* Corresponding Author: msafakamer@ksu.edu.tr

(Received: 16.03.2022; Revised: 23.05.2022; Accepted: 03.09.2022)

ABSTRACT

Today, 3D manufacturing technologies are shown as candidates to replace traditional manufacturing technologies. In this direction, many studies are carried out to reduce the disadvantages of 3D manufacturing technologies. The first few of these disadvantages are; high production cost, slow production speed, and lower strength values of the produced product compared to traditional methods. Increasing or decreasing the printing speed, which is one of the 3d production parameters, appears as a parameter that will directly affect the strength and production costs of the produced product. For this reason, it is important to determine the effects that may occur on the mechanical properties of the product produced by changing the printing speed in terms of choosing the printing speed according to the intended use of the product. In this study, the effect of desktop Fused Deposition Modelling (FDM) 3D printing speed on mechanical properties was investigated. Tensile test samples were produced using Polylactic Acid (PLA) material at seven different printing speeds using two different 3D printers operated without bed heating. The mass, hardness, surface roughness, and porosity values of the produced samples were determined. Fractured surfaces of the samples were analyzed using Scanning electron microscopy (SEM) images. The results show that an increase in the printing speed decreases the mass, the top surface hardness, and the tensile strength and increases the porosity, the arithmetic average roughness of the products produced with both 3D printers.

Keywords: 3D Printing, Additive Manufacturing, Fused Deposition Modeling, Scanning Electron Microscopy, Tensile Test.

1. INTRODUCTION

3D printing technology; has become more and more important today with its capabilities that reduce design constraints, minimize production waste, and rapidly prototype complex designs. Designing and manufacturing functional parts for various different fields such as engineering and medicine is an important goal of this technology [1, 2]. Many approaches in this area also offer innovative applications in design for additive manufacturing. For example, production with fused deposition modeling (FDM) technology has advantages such as cheap machinery and materials. However, the FDM technology has limited mechanical properties, and new technical approaches are

needed to overcome these limitations [3-9]. In this direction, it is necessary to focus on studies to increase the intralayer and interlayer bonds in the products produced with FDM.

Many studies have been carried out to determine the various properties of products produced with 3D printers using the FDM method [10-15]. Sood et al. [16] investigated the effects of layer thickness, scanning angle, scanning width, orientation, and air gap parameters on the tensile, flexural, and impact strength of test specimens. They conducted experiments based on central composite design (CCD) to reduce experimental runs. They developed empirical models relating to

response and process parameters. They tested the validity of the models using the analysis of variance (ANOVA) statistical approach. They found that the full quadratic model with a regression p-value less than 0.05 and a lack of fit of more than 0.05 was suitable for tensile strength, flexural strength, and impact strength. Chacon et al. [17] investigated the effect of printing direction, layer thickness, and feed rate on test samples produced using a 3D printer and Polylactic Acid (PLA) material. They performed tensile and 3-point bending tests to determine the effects on the test specimens. The test samples displayed anisotropic behavior due to the layer-by-layer printing. They determined that the samples that produced vertical orientation to the print direction had the lowest mechanical properties. In addition, they found that ductility decreases with the increase in layer thickness and printing speed. Solmaz and Celik [18] investigated the behavior of honeycomb sandwich composites produced using a 3D printer under compression load. They used Acrylonitrile Butadiene Styrene (ABS) and PLA filament in the production of honeycomb cells with three different cell sizes and cell heights. They determined that the critical buckling loads of the samples obtained from PLA material were higher than those produced using ABS material. Tatlı and Ozgul [19] designed and manufactured a 3D FDM printer with a 200x200x210 mm printing volume. They produced test samples using the in-house built 3D printer with two different internal infill patterns (gyroid, grid) using PLA material to study tensile, 3-point bending, and impact properties of the produced samples. They determined that the samples produced with the grid infill pattern have maximum tensile strength, and those produced with the gyroid infill pattern have the maximum bending strength. They concluded that these two infill patterns did not significantly affect Charpy impact strength. Gupta et al. [20] investigated the effect of heat treatment on the mechanical strength of FDM 3D-printed PLA parts with constant 3D printing parameters and ambient conditions. They compared the heat-treated set of samples at a specific temperature for 1 hour and cooled them in the furnace with another set of untreated samples. They determined that the mechanical properties improved by 4.88 % to 10.26 % at a maximum heat treatment of 110 °C and below the recrystallization temperature of 65 °C. Torun et al. [21] investigated the effects

of various filling ratios on the fracture toughness of 3D-printed PLA samples with gyroid patterns using numerical simulation and experimental work. They created two-dimensional finite element modeling and extracted two-dimensional functions of the stress density coefficients of the gyroid PLA samples at various filling ratios. They determined that the amount of fracture toughness of the samples in the tensile mode was much higher than the values in the shear mode. They also found that both tensile and shear fracture toughness improved as the percentages of filling ratios in the samples increased.

Various composite materials can also be produced using 3D printing technology. Some of the studies carried out to determine the mechanical properties of composite materials produced using 3D printers are given below. Ning et al. [22] experimentally investigated the effects of sweep angle, filling speed, nozzle temperature, and layer thickness on the tensile strength of Carbon Fiber Reinforced Plastic (CFRP) composites produced by the FDM method. They examined the SEM images of the fracture surfaces of CFRP composite materials fractured in tensile tests. They determined that tensile strength decreases with increasing printing speed. Kumar et al. [23] applied Al metal powder reinforcement, which provides better mixing during Friction Stir Welding (FSW), to polymer materials to solve the problems preventing two different polymers (ABS and PA6) from joining with the required size FSW. They used Twin Screw Extrusion (TSE) and melt deposition modeling to prepare the samples ABS-15Al and PA6-50Al. They performed multi-factor optimization to select the best set of process parameters and determined that the reinforcement made caused the material to be thermally compatible with each other for FSW application. Roj et al. [24] compared tensile specimens produced with FDM, printed in three orientations, with compression-molded components. In addition to ordinary filaments, composite materials with metal, carbon, wood, and stone additives were also investigated. As a result, they determined that the mechanical properties depend on the densities of the components. Uzun and Erdogdu [25] produced 20 % copper reinforced and 20 % carbon-fiber-reinforced PLA composites and bare samples with a 3D printer. They compared

their mechanical properties by subjecting the samples they produced to the tensile test and the three-point bending test. They determined that adding copper and carbon fiber reinforcements to PLA material reduces tensile and bending strengths. Ando et al. [26] investigated the interface adhesion properties of parts made of PLA in different colors produced by FDM technology. They first glued the test samples they prepared with different contact surface types and then applied the tensile test. They used two other methods for bonding FDM specimens as vertical adhesion and horizontal adhesion. They found that vertical adhesion was always weaker than horizontal adhesion.

To the best of the author's knowledge, there is no study comparing the mechanical properties of tensile test specimens produced at different printing speeds with Ultimaker 2 Go (U2G) and Ultimaker 2 Extended (U2E) 3D printers in the literature. This study produced tensile test samples using PLA material at different printing speeds (20-40-60-80-100-120-140 mm/s) with U2G and U2E 3D printers without using bed heating. The effect of printing speed on mechanical properties was investigated. The mass, hardness, and surface roughness of the produced samples were measured, porosity values were calculated, and the samples produced were tensile tested. After the tensile test, SEM images of the fractured samples were taken from the fracturing regions. Mechanical properties of samples produced with the same parameters in both 3D printers were compared.

2. MATERIAL AND METHOD

U2G [27, 28] and U2E [29, 30] 3D printers were used in the production of test samples. Standard ASTM D638-14 [31] was used for sizing the tensile specimens. In this standard, samples were produced in Type IVB dimensions (Figure 1) that can fit on the printing bed of both 3D printers. The tensile sample with the specified standard dimensions was designed 3D in a computer environment using SolidWorks CAD software. Cura CAM software, the software of the Ultimaker 3D printer, was used in creating G-codes by selecting the parameters specified in Table 1. The code defines settings, such as the design's position, angle, etc., on the printer bed. The generated G-codes were transferred to the 3D printer using an SD card input. The parameters in Table 1 are the default settings when the infill density is 100 % selected.

The print bed was manually calibrated on both 3D printers. Ultimaker PLA orange material [32, 33] was installed in the 3D printer. The printing bed temperature of 3D printers was set to 0 °C. In this case, it can be assumed that the printing bed was at ambient temperature, as it did not have any cooling system. The nozzle temperature of both 3D printers was set to 230 °C (195-240 °C temperature range specified on the Ultimaker PLA material product label). Before starting the production process, a thin film layer thickness of glue stick (Uhu Stic Magic Blue) was applied to the printing bed to ensure better adhesion of the first layer of the sample to the glass printing bed during production.

The default printing speed in the 3D printers used in this study is 60 mm/s. Without changing other printing parameters, this study started with the minimum and maximum printing speeds that 3D printers can reach determined. Since a sudden mass loss and increase in porosity were observed in the samples produced with a printing speed of 140 mm/s, the printing speed was not increased any further. Tensile samples were produced at seven different printing speeds (20-40-60-80-100-120-140 mm/s). A total of 42 tensile samples were produced, 3 for each printing speed and 21 for each printer. The mass, hardness, and surface roughness of the tensile samples produced were measured, and tensile tests were performed on the samples. After the tensile test, SEM images of the fractured samples were taken from the fracturing regions. Mass measurements were made with a precision balance of KERN PLS 6200-2A (capacity: 6.200 g, precision: 0.01 g). Hardness measurements were taken from 5 different points on the top surface and bottom surface of each sample in Shore D with the MITECH MH210 portable hardness tester. The averaged hardness values were used for comparison. Surface roughness measurements were taken using the JENOPTIK Hommel-Etamic W5 surface roughness measuring device at the parameters given in Table 2. Measurements were taken from the top surface of each sample. The roughness device was positioned on the top surface parallel to the deposition direction, 45° to the deposition direction, and 90° to the deposition direction, and average values were determined by measuring at three different points for each situation. Tensile tests were performed with a

100 kN capacity Zwick/Roell Z100 tensile tester at 5 mm/min speed and using ASTM D638-14 standard. Images of fractured regions

of samples fractured in tensile tests were taken with the ZEISS EVO LS 10 SEM.

Table 1. Selected parameters in Cura CAM software.

3D Printer	Ultimaker 2 go/Ultimaker 2 extended with olsson block
Material	Ultimaker PLA orange 2.85 mm
Nozzle diameter	0.4 mm
Layer thickness	0.2 mm
Wall thickness	0.8 mm
Top/Bottom thickness	0.8 mm
Infill density	100 %
Infill pattern	Lines
Print speed	20-40-60-80-100-120-140 mm/s
Travel speed	(Test samples have been produced at seven different printing speeds) 120 mm/s

Table 2. Parameters of surface roughness measurement.

Measuring length (lt)	4.8 mm
Measurement speed (vt)	0.5 mm/s
Wavelength (lc)	0.8 mm

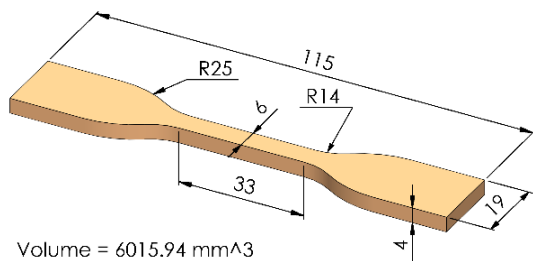


Figure 1. Standard of ASTM D638-14 Type IV^B.

3. RESULTS AND DISCUSSIONS

In this study, the effect of printer type and printing speed on the mechanical properties of test specimens produced in two different printers using PLA material was investigated. U2G and U2E were used as 3D printer types. Bed heating was not used in the production of test samples.

3.1. Mass and Porosity Values of Samples

The mass changes of the products according to the printing speeds are shown in Figure 2a. It can be said that the masses of the products produced with the U2E 3D printer decrease with the increase in printing speed, and this decrease shows an almost linear change. However, when the graphic was examined, it was seen that the mass of the products produced with the U2G 3D printer decreased irregularly with the increase in printing speed. The filament length data obtained from the Cura CAM program were the same for all samples. This means that the amount of material required for printing

calculated in the program must be the same at all printing speeds. However, when Figure 2a was examined, it was seen that as the printing speed increased, the mass of the produced samples decreased in both printers. This difference was thought to be due to the filament feeding motor of the 3D printer. It was thought that with the increase in printing speed, the filament feeding motor was insufficient to feed the filament required for printing. As a result of this situation, gaps occurred in some zones of the printed test samples. When the test sample masses measured according to printing speeds were compared for both printers, it was seen that the masses of the samples produced with the U2E 3D printer were greater than the masses of the samples produced with the U2G 3D printer. From this, it can be concluded that the filament feeding motor of the U2E 3D printer provides the required filament better for printing.

Another parameter related to the products produced with a 3D printer is porosity. Porosity can be expressed as the ratio of the gap volume in the manufactured product to the total volume of the design (Equation 1). The gap volume in a product produced with a 3D printer; can be calculated by subtracting the print volume corresponding to the mass of the product produced from the total volume of the design (Equation 2). The printing volume corresponding to the mass of the product produced by the 3D printer can be calculated by dividing the mass of the product produced by the 3D printer by the density of the filament material used in production (Equation 3).

$$\phi = \frac{V_b}{V_T} \cdot 100 \tag{1}$$

$$V_b = V_T - V_p \tag{2}$$

$$m = \rho \cdot V_p \Rightarrow V_p = \frac{m}{\rho} \tag{3}$$

Here;

ϕ : the porosity,

V_b : the gap volume inside the product produced with a 3D printer,

V_T : the total volume of the design,

V_p : the printing volume corresponding to the mass of the product produced with a 3D printer,
 m : the mass of the product produced with a 3D printer,

ρ : the density of the filament material used in production expresses.

Using the equations above, the porosity values of the products produced at different printing speeds with both 3D printers were calculated. The total volume of the test specimen design was taken from the SolidWorks program, where the design was made (Figure 1). In addition, the density of Ultimaker PLA Orange filament material used in production was taken from the PLA filament catalogs of the Ultimaker brand [32, 33]. The calculations were made assuming that there was no density change in the PLA material during printing.

Using the values calculated for both 3D printers, a graph showing the change of porosity values of the produced test samples with the printing speed was drawn (Figure 2b). From Figure 2b, it can be said that the porosity values of the products produced with the U2E 3D printer increased with the increase in printing speed, and this increase shows an almost linear change. However, it was seen that the porosity values of the products produced with the U2G 3D printer increase irregularly with the increase of printing speed. The increase in the porosity values of the products produced with PLA material with the increase in printing speed was in harmony with similar studies in the literature [34]. Moreover, it was seen that among the porosity values corresponding to the same printing speeds, the porosity values of the products produced with the U2E 3D printer were lower.

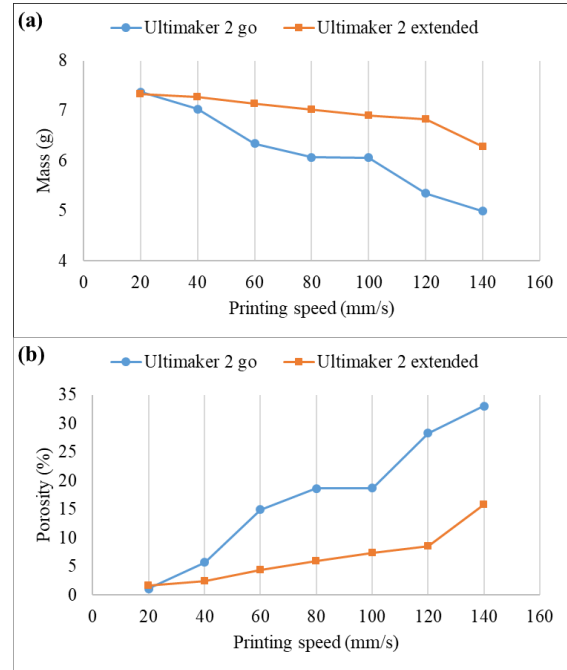


Figure 2. The curves show the change of (a) mass and (b) porosity according to printing speed.

3.2. Hardness Values of Samples

Shore D hardness values of test samples are given in Table 3. The hardness of the top and bottom surfaces of each sample was measured. It was determined that the hardness values on the top surfaces decrease with the increase of the printing speed. As the printing speed increased, it was observed that the filament feeding motor was insufficient to feed the filament required for printing, and irregular gaps inside the layer were formed in the test samples. It can be said that the difference in some values seen in the table was due to regional gaps in test samples. As seen in Table 3, it was seen that the bottom surface hardness of the samples was generally higher than the top surface hardness. Similar results were found in the literature [35]. The bottom surfaces of the samples were in contact with the glass printing bed, and some adhesive residue remains on the bottom surfaces of the samples after production. It was thought that the adhesive applied on the printing bed in a thin film thickness to ensure better adhesion of the first layer of the sample to the glass printing bed caused the hardness of the bottom surfaces of the samples to increase. When the test sample surface hardnesses measured according to printing speeds were compared for both printers, it was seen that the samples produced with the U2E 3D printer were harder than the samples produced with the U2G 3D printer.

Table 3. The hardness of test samples.

Printing speed (mm/s)	Shore D hardness values HS			
	Ultimaker 2 go		Ultimaker 2 extended	
	Top surface	Bottom surface	Top surface	Bottom surface
20	67.47	55.67	68.03	66.13
40	59.73	61.10	65.90	62.50
60	47.87	66.53	64.33	57.80
80	49.70	59.10	56.83	60.73
100	44.90	62.00	58.27	60.90
120	46.97	60.07	52.17	57.30
140	52.00	59.93	51.97	60.37

3.3. Roughness Values of Samples

The arithmetic average roughness values of the top surfaces of the test samples are given in Table 4. It can be seen that the arithmetic average roughness values generally increase with the increase in printing speed. It should be noted that the difference in some values seen in the table was due to regional gaps in test samples. When the surface roughness was examined according to the deposition direction, it was seen that the lowest roughness values were in the measurements made parallel to the deposition direction at all printing speeds, and the highest roughness values were in the measurements made at an angle of 90° to the

deposition direction. These results were expected before production. When the test sample surface roughnesses measured according to printing speeds were compared for both printers, it was seen that the surface roughness of the samples produced with the U2E 3D printer was much lower than the samples produced with the U2G 3D printer. In addition, with the increase in printing speed, there was a slight increase in the roughness values of the samples produced with the U2E 3D printer, while the roughness values of the samples produced with the U2G 3D printer increased to a larger extent.

Table 4. Roughness values of test samples.

Printing speed (mm/s)	Arithmetic average roughness, Ra (µm)					
	Ultimaker 2 go			Ultimaker 2 extended		
	Parallel	45° angle	90° angle	Parallel	45° angle	90° angle
20	2.514	5.182	5.991	0.782	2.363	3.097
40	1.157	6.211	6.382	0.954	4.293	5.360
60	2.108	14.417	16.448	0.791	4.320	5.402
80	1.255	11.925	13.294	1.003	4.773	5.106
100	1.408	17.304	20.043	1.015	6.155	6.885
120	1.504	18.343	21.402	0.923	6.157	7.442
140	4.018	14.330	15.605	1.073	9.951	10.116

3.4. Tensile Test Results

For both 3D printers, a graph showing the change of the tensile strength values of the produced test samples with the printing speed was produced and given in Figure 3a. It can be seen from Figure 3a that the tensile strength values of the products produced by both 3D printers decrease as the printing speed increases, and this change is almost linear. There were similar studies in the literature showing that the tensile strength of the products produced with PLA material decreases with the increase in printing speed [34-36]. Again from the same Figure, the tensile strength values corresponding to the same printing speeds are almost the same in both 3D printers at 20 mm/s

printing speed, and the tensile strength values range of the products produced with both 3D printers gradually expands with the increase in printing speed. When the tensile strength of the samples was compared for both printers according to the printing speeds, it was seen that the tensile strength of the samples produced with the U2E 3D printer was higher than the samples produced with the U2G 3D printer.

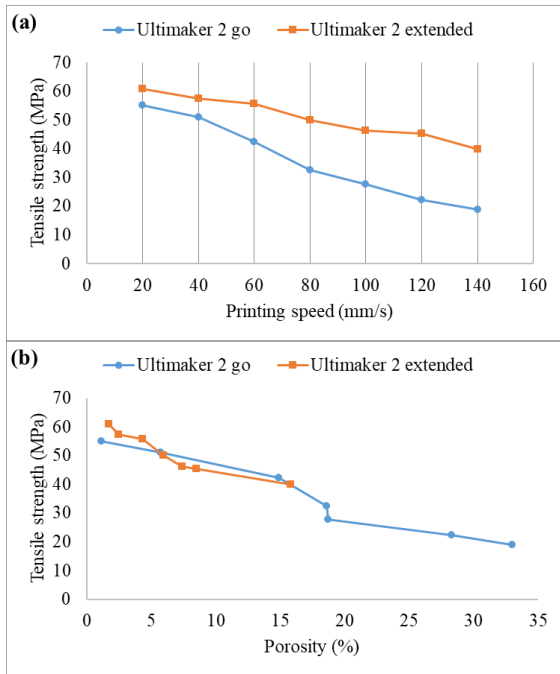


Figure 3. Change of test samples tensile strength values produced with different printers with (a) printing speed and (b) porosity.

A graph showing the change of tensile strength values with porosity of the test samples produced with both 3D printers at different printing speeds was drawn (Figure 3b). It can be seen from Figure 3b that the tensile strength values of the products produced with both 3D printers decreased with the increase of porosity values, and this change was almost linear. In addition, it was determined that the tensile strength values corresponding to the same porosity values of the test samples in the graphic were close to each other in both 3D printers.

In Figure 4, the stress-strain curves of the samples produced with both 3D printers at different printing speeds are given. When Figure 4a was examined, it was determined that the highest fracture strain values among the samples produced with the U2G 3D printer at different printing speeds were found in the samples produced at 60, 80, and 100 mm/s printing speeds. It was determined that among the samples with the highest fracture strain values, the sample with the highest tensile strength was at 60 mm/s printing speed. In addition, it was determined that the highest tensile strengths were found in samples produced at 20 and 40 mm/s printing speeds.

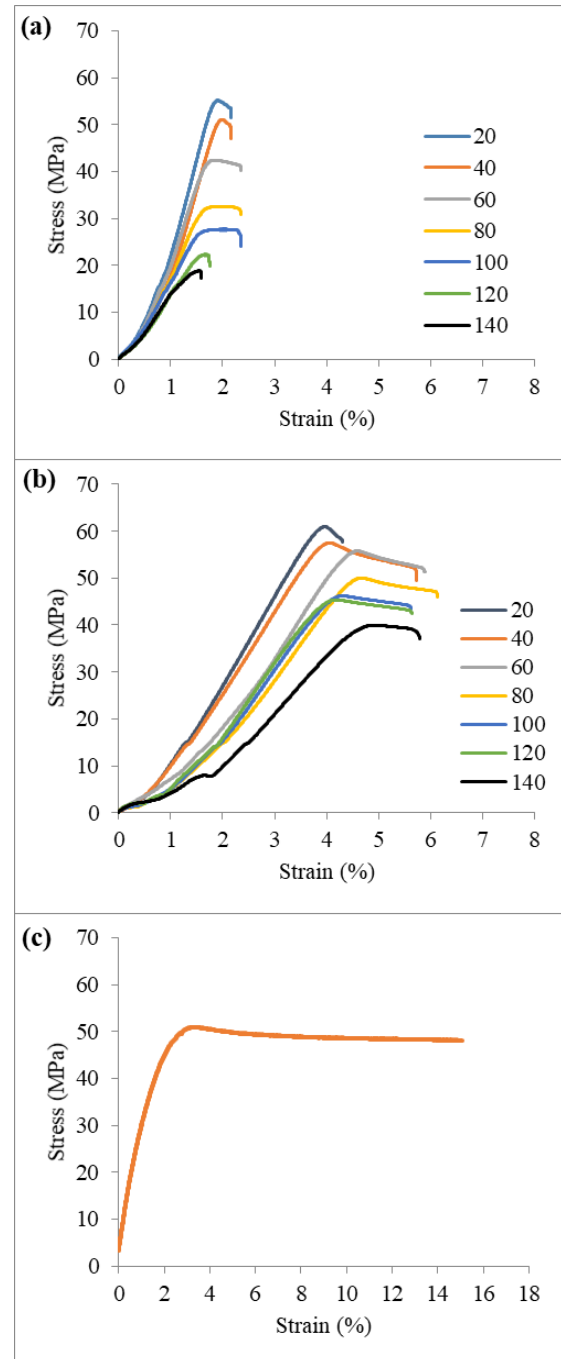


Figure 4. Stress-strain curves (a) samples produced with Ultimaker 2 Go 3D printer, (b) samples produced with Ultimaker 2 Extended 3D printer, and (c) Ultimaker PLA Orange 2.85mm filament.

When Figure 4b was examined, it was determined that the highest fracture strain values among the samples produced with the U2E 3D printer at different printing speeds were found in the samples produced at 40, 60, and 80 mm/s printing speeds. It was also determined that the sample produced at 40 mm/s printing speed has the highest strain at fracture and tensile strength. In addition, the highest tensile strengths were found in samples produced at 20

and 40 mm/s printing speeds. Hooke lines of samples produced at printing speeds of 60, 80, 100, and 120 mm/s were almost coincident with each other. Among these samples printed with 60, 80, 100, and 120 mm/s speed, it was seen that the sample at 60 mm/s printing speed has the highest tensile strength. When the stress-strain curves of the samples produced with both 3D printers at different printing speeds were compared, it was seen that the highest tensile strength and the highest elongation values were in the samples produced with the U2E 3D printer.

The tensile test was also applied to the Ultimaker PLA Orange 2.85 mm filament used for printing samples produced by both 3D printers, and the stress-strain curve of the tensile test of this filament was given in Figure 4c. When the stress-strain curves shown in Figure 4 was examined, it was seen that the fracture strain of the Ultimaker PLA Orange 2.85 mm filament was much higher than the elongation values of the test specimens produced by both 3D printers. According to this result, it can be said that the fracture strain of the Ultimaker PLA Orange 2.85 mm filament material used in the printing process was considerably reduced as a result of the printing process.

From Figure 4c, the effective Young's modulus of Ultimaker PLA Orange 2.85 mm filament used in the printing process was approximately 2 GPa. When Figure 4 was examined, it was seen that the effective Young's modulus of the products produced with the U2G 3D printer was approximately 1 GPa, and the effective Young's modulus of the products produced with the U2E 3D printer was 0.5 GPa on average. In line with these data, it was determined that the effective Young's modulus of the PLA samples decreased after the printing process. In addition, with the increase in printing speed, the effective Young's modulus of the products produced in both 3D printers also decreased. When the effective Young's modulus of the samples produced with both 3D printers at different printing speeds was compared, it was seen that the effective Young's modulus of the samples produced with the U2E 3D printer was lower.

Again from Figure 4, the toughness of the PLA material decreases, and the material becomes brittle after the printing process. It was

determined that the printing process reduces the deformability of the PLA material. In addition, with the increase in printing speed, the toughness of the products produced in both 3D printers has decreased among themselves. When samples produced with both 3D printers at different printing speeds were compared, it was found that the products produced with the U2G 3D printer became more fragile.

3.5. SEM Images of The Fractured Regions of Samples

After the tensile test, pictures of the fractured regions of the fractured test samples were taken with a 100 times magnification in the SEM and were given in Figure 5. It can be seen from the figure that there is almost no gap in each layer of the samples produced with 20 mm/s printing speed in both 3D printers. The gaps between the 3D printed fibers in each layer of the samples produced increase with the increase of printing speed.

When the samples produced with the U2G 3D printer were examined, it was seen that the 3D printed fibers in each layer were in linear contact with each other in the samples with 40 and 60 mm/s printing speeds. It was seen that in the samples with printing speeds of 80 mm/s and higher on the same printer, the interlayer gaps increase even more, and the 3D printed fibers in each layer do not touch each other.

When the samples produced with the U2E 3D printer were examined, it was seen that the 3D printed fibers in each layer were in linear contact with each other in the samples with 100 and 120 mm/s printing speeds. In the samples with a printing speed of 140 mm/s on the same printer, the interlayer gaps increased even more, and the 3D printed fibers in each layer do not touch each other.

When the fractured regions of the samples produced with both 3D printers at different printing speeds were compared with the 100 times magnified images in SEM, it was seen that the interlayer gaps were much higher in the samples produced with the U2G 3D printer at the same printing speed. All these findings confirm our determination that the filament feeding motor was insufficient to feed the filament required for printing as the printing speed increases.

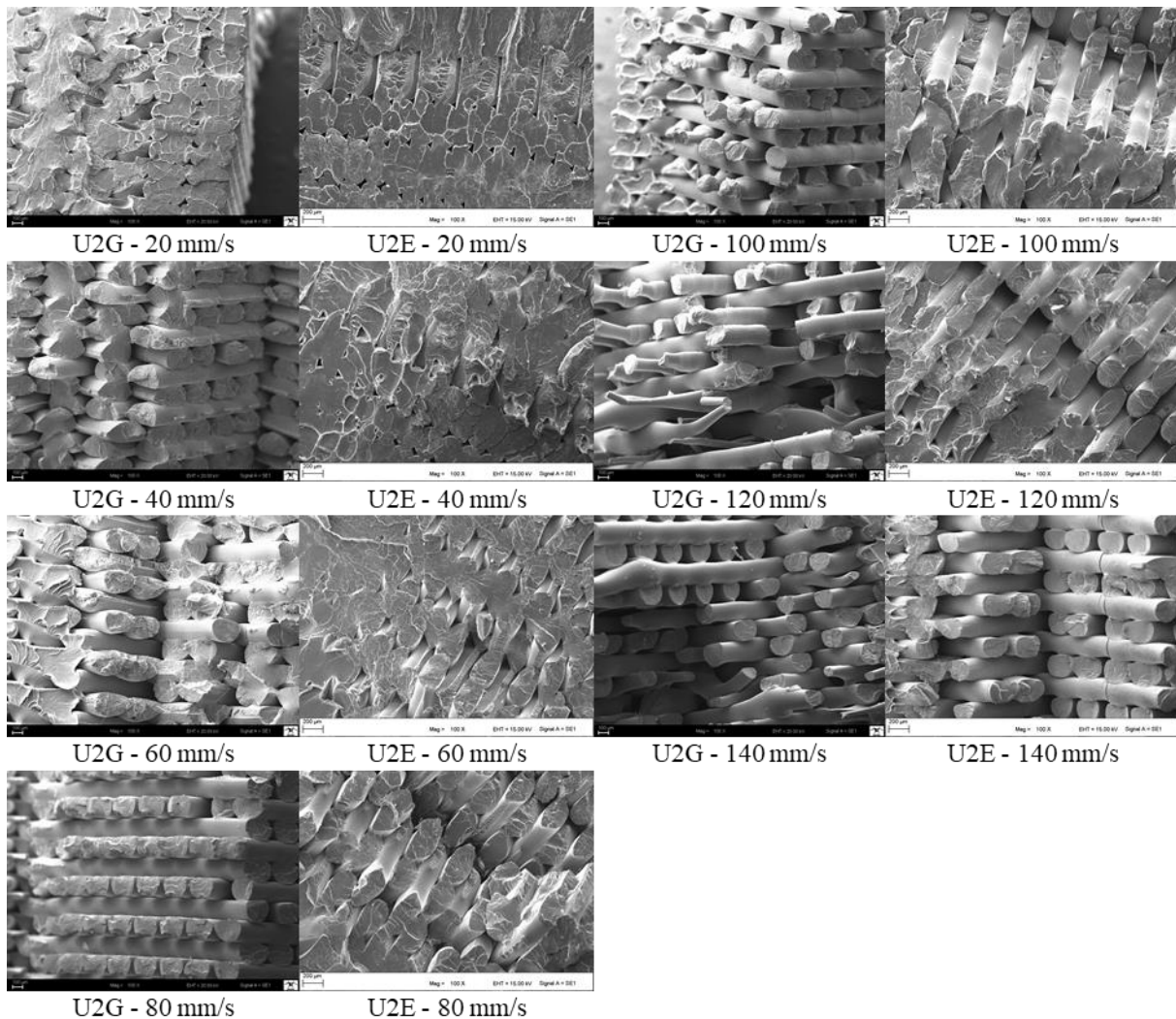


Figure 5. 100 times magnified images taken from SEM of the fractured regions of samples produced at different printing speeds.

4. CONCLUSIONS

In this study, tensile samples were produced using PLA material at different printing speeds using commercial desktop U2G and U2E 3D printers. Mechanical properties of test samples produced with the same parameters in both 3D printers were compared. Results show that an increase in the printing speed decreases the mass, the top surface hardness, and the tensile strength and increases the porosity, the arithmetic average roughness of the products produced with both 3D printers. It was determined that the effective Young's modulus of the PLA material was decreased after printing. In addition, the effective Young's modulus of the products produced in both 3D printers decreases with the increase in printing speed. After printing, it was observed that the toughness of the PLA material decreased, and the material became brittle. It was also determined that the printing process reduces the

deformability of the PLA material. In addition, the toughness of the products produced in both 3D printers has decreased with the increase in printing speed. As a general conclusion, it was found that products produced with U2E 3D printers have superior mechanical properties than products produced with U2G 3D printers.

4.1. Recommendations for Future Work

Irregularities that occur with the increase in printing speed are, in some cases, caused by the filament feeding system and, in some cases, by the inability to provide the required nozzle temperature for melting according to the selected printing speed. In case of changing the printing speed in future studies, printing speed studies can be done with 3D printers where the filament feeding engine can provide the required filament, and the printing nozzle can also provide the appropriate melting

temperature for the printing speed manually or automatically.

ACKNOWLEDGES

This work; was supported by the Scientific Research Projects Coordination Unit of the Rectorate of Inonu University with the project number FDK-2020-2351. We would like to thank Inonu University for its valuable contributions.

REFERENCES

1. Ngo, T.D., Kashani, A., Imbalzano, G., Nguyen, K.T.Q., Hui, D., "Additive manufacturing (3D printing): A review of materials, methods, applications and challenges", *Composite Part B: Engineering*, Vol. 143, Pages 172-196, 2018.
2. Popescu, D., Zapciu, A., Amza, C., Baci, F., Marinescu, R., "FDM process parameters influence over the mechanical properties of polymer specimens: A review", *Polymer Testing*, Vol. 69, Pages 157-166, 2018.
3. Yaman, U., Butt, N., Sacks, E., Hoffmann C., "Slice coherence in a query-based architecture for 3D heterogeneous printing", *Computer-Aided Design*, Vol. 75-76, Pages 27-38, 2016.
4. Beran, T., Mulholland, T., Henning, F., Rudolph, N., Osswald, T.A., "Nozzle clogging factors during fused filament fabrication of spherical particle filled polymers", *Additive Manufacturing*, Vol. 23, Pages 206-214, 2018.
5. Osswald, T.A., Puentes, J., Kattinger, J., "Fused filament fabrication melting model", *Additive Manufacturing*, Vol. 22, Pages 51-59, 2018.
6. Yaman, U., "Shrinkage compensation of holes via shrinkage of interior structure in FDM process", *The International Journal of Advanced Manufacturing Technology*, Vol. 94, Pages 2187-2197, 2018.
7. Dilberoglu, U.M., Simsek, S., Yaman, U., "Shrinkage compensation approach proposed for ABS material in FDM process", *Materials and Manufacturing Processes*, Vol. 34, Pages 993-998, 2019.
8. Mazzei Capote, G.A., Rudolph, N.M., Osswald, P.V., Osswald, T.A., "Failure surface development for ABS fused filament fabrication parts" *Additive Manufacturing*, Vol. 28, Pages 169-175, 2019.
9. Graziosi, S., Cannazza, F., Vedani, M., Ratti, A., Tamburrino, F., Bordegoni, M., "Design and testing of an innovative 3D-printed metal-composite junction" *Additive Manufacturing*, Vol. 36, Issue 101311, Pages 1-18, 2020.
10. Kamer, M.S., Doğan, O., Temiz, Ş., Yaykaşlı, H., "3 Boyutlu yazıcı ile farklı yazdırma parametreleri kullanılarak üretilen eğme test numunelerinin mekanik özelliklerinin incelenmesi" [Investigation of the mechanical properties of flexural test samples produced using different printing parameters with a 3D printer], *Cukurova University Journal of the Faculty of Engineering*, Vol. 36, Issue 3, Pages 835-846, 2021.
11. Kamer, M.S., Temiz, Ş., "3 Boyutlu yazıcıda ABS ve PLA filamentler ile farklı tabla ve nozul sıcaklıkları kullanılarak üretilen çekme test numunelerinin mekanik özelliklerinin araştırılması" [Investigation of the mechanical properties of tensile test samples produced with a 3D printer using different bed and nozzle temperatures with ABS and PLA filaments], *Kahramanmaraş Sütçü İmam Üniversitesi Mühendislik Bilimleri Dergisi*, Vol. 24, Issue 4, Pages 341-358, 2021.
12. Kamer, M.S., Temiz, Ş., Yaykaşlı, H., Kaya, A., "3 Boyutlu yazıcı ile farklı renklerde ve farklı dolgu desenlerinde üretilen çekme test numunelerinin mekanik özelliklerinin incelenmesi" [Investigation of the mechanical properties of tensile test samples produced in different colors and different infill patterns with a 3D printer], *Uludağ University Journal of the Faculty of Engineering*, Vol. 26, Issue 3, Pages 829-848, 2021.
13. Karabeyoglu, S.S., Eksi, O., Yaman, P., Kucukyildirim, B.O., "Effects of infill pattern and density on wear performance of FDM-printed acrylonitrile-butadiene-styrene parts", *Journal of Polymer Engineering*, Vol. 41, Issue 10, Pages 854-862, 2021.
14. Tognana, S., Montecinos, S., Gastien, R., Salgueiro, W., "Influence of fabrication parameters on the elastic modulus and characteristic stresses in 3D printed PLA samples produced via fused deposition modelling technique", *Journal of Polymer Engineering*, Vol. 41, Issue 6, Pages 490-498, 2021.
15. Dobos, J., Hanon, M.M., Oldal, I., "Effect of infill density and pattern on the specific load capacity of FDM 3D-printed PLA multi-layer sandwich", *Journal of Polymer Engineering*, Vol. 42, Issue 2, Pages 118-128, 2022.
16. Sood, A.K., Ohdar, R.K., Mahapatra, S.S., "Parametric appraisal of mechanical property of fused deposition modelling processed parts" *Materials Design*, Vol. 31, Issue 1, Pages 287-295, 2010.
17. Chacon, J.M., Caminero, M.A., Garcia-Plaza, E.,

- Nunez, P.J., “Additive manufacturing of PLA structures using fused deposition modelling: Effect of process parameters on mechanical properties and their optimal selection”, *Materials Design*, Vol. 124, Pages 143-157, 2017.
18. Solmaz, M.Y., Çelik, E., “3 Boyutlu yazıcı kullanılarak üretilen bal peteği sandviç kompozitlerin basma yükü altındaki performanslarının araştırılması” [Investigation of compression test performances of honeycomb sandwich composites produced by 3d printing method], *Firat University Journal of Engineering Sciences*, Vol. 30, Issue 1, Pages 277-286, 2018.
19. Ozgul, H.G., Tatli, O., “3D Printer Design, Manufacturing and Effect of Infill Patterns on Mechanical Properties”, *Icontech International Journal*, Vol. 4, Issue 1, Pages 13-24, 2020.
20. Gupta, P., Kumari, S., Gupta, A., Sinha, A.K., Jindal, P., “Effect of heat treatment on mechanical properties of 3D printed polylactic acid parts” *Materials Testing*, Vol. 63, Issue 1, Pages 73-78, 2021.
21. Torun, A.R., Dike, A.S., Yildiz, E.C., Saglam, İ., Choupani, N., “Fracture characterization and modeling of Gyroid filled 3D printed PLA structures”, *Materials Testing*, Vol. 63, Issue 5, Pages 397-401, 2021.
22. Ning, F., Cong, W., Hu, Y., Wang, H. J., “Additive manufacturing of carbon fiber-reinforced plastic composites using fused deposition modeling: Effects of process parameters on tensile properties”, *Journal of Composite Materials*, Vol. 51, Issue 4, Pages 451-462, 2017.
23. Kumar, R., Singh, R., Ahuja, I., “Friction stir welding of ABS-15Al sheets by introducing compatible semi-consumable shoulder-less pin of PA6-50Al”, *Measurement*, Vol. 131, Pages 461-472, 2019.
24. Roj, R., Nurnberg, J., Theiss, R., Dultgen, P., “Comparison of FDM-printed and compression molded tensile samples”, *Materials Testing*, Vol. 62, Issue 10, Pages 985-992, 2020.
25. Uzun, M., Erdoğan, Y., “Eriyik yığma modellemesi ile üretimde takviyesiz ve takviyeli PLA kullanımının mekanik özelliklere etkisinin araştırılması” [Investigation of the effect of using unreinforced and reinforced PLA in production by fused deposition modeling on mechanical properties], *Iğdır Üniversitesi Fen Bilimleri Enstitüsü Dergisi*, Vol. 10, Issue 4, Pages 2800-2808, 2020.
26. Ando, M., Biroş, M., Jeganmohan, S., “Surface bonding of additive manufactured parts from multi-colored PLA materials”, *Measurement*, Vol. 169, Issue 108583, Pages 1-7, 2021.
27. Ultimaker, “The Ultimaker 2 Go specifications”, <https://support.ultimaker.com/hc/enus/articles/360011935299-The-Ultimaker-2-Go-specifications>, February 06, 2021.
28. Ultimaker, “The Ultimaker 2 Go user manual”, <https://support.ultimaker.com/hc/enus/articles/360011813180-The-Ultimaker-2-Go-user-manual>, February 06, 2021.
29. Ultimaker, “The Ultimaker 2 Extended specifications”, <https://support.ultimaker.com/hc/enus/articles/360011987939-The-Ultimaker-2-Extended-specifications>, February 06, 2021.
30. Ultimaker, “The Ultimaker 2 Extended user manual”, <https://support.ultimaker.com/hc/enus/articles/360011987819-The-Ultimaker-2-Extended-user-manual>, February 06, 2021.
31. Standard ASTM D638-14, “Standard Test Method for Tensile Properties of Plastics”, 2014.
32. Ultimaker, “Ultimaker PLA SDS”, <https://support.ultimaker.com/hc/enus/articles/360012759359-Ultimaker-PLA-SDS>, February 06, 2021.
33. Ultimaker, “Ultimaker PLA TDS”, <https://support.ultimaker.com/hc/enus/articles/360011962720-Ultimaker-PLA-TDS>, February 06, 2021.
34. Tao, Y., Li, P., Pan, L., “Improving tensile properties of polylactic acid parts by adjusting printing parameters of open source 3D printers”, *Material Science*, Vol. 26, Issue 1, Pages 83-87, 2020.
35. Aydın, M., Yıldırım, F., Çantı, E., “Farklı yazdırma parametrelerinde PLA filamentin işlem performansının incelenmesi” [Investigation of the processing performance of PLA filament in different printing parameters], *International Journal of 3D Printing Technologies and Digital Industry*, Vol. 3, Issue 2, Pages 102-115, 2019.
36. Gunay, M., “Modeling of Tensile and Bending Strength for PLA Parts Produced by FDM”, *International Journal of 3D Printing Technologies and Digital Industry*, Vol. 3, Issue 3, Pages 204-211, 2019.